Environmental Science & Technology

Article

pubs.acs.org/est

Recent Transport History of Fukushima Radioactivity in the Northeast Pacific Ocean

John N. Smith,*[,†] Vincent Rossi,[‡,§] Ken O. Buesseler,[∥] Jay T. Cullen,[⊥] Jack Cornett,[#] Richard Nelson,[†] Alison M. Macdonald,[∥] Marie Robert,[▽] and Jonathan Kellogg[⊥]

[†]Bedford Institute of Oceanography, Fisheries and Oceans Canada, Dartmouth, Nova Scotia B2Y 4A2, Canada

[‡]Mediterranean Institute of Oceanography (UM 110, UMR 7294), CNRS, Aix Marseille Université, Université Toulon, IRD, 13288 Marseille, France

[§]Climate Change Research Centre, University of New South Wales, Sydney, New South Wales 2052, Australia

[∥]Woods Hole Oceanographic Institute, Woods Hole, Massachusetts 02543-1050, United States

[⊥]University of Victoria, Victoria, British Columbia V8P 5C2, Canada

[#]University of Ottawa, Ottawa, Ontario K1N 6N5, Canada

[▽]Institute of Ocean Sciences, Fisheries and Oceans Canada, Sidney, British Columbia V8L 4B2, Canada

ABSTRACT: The large inventory of radioactivity released during the March, 2011 Fukushima Dai-ichi nuclear reactor accident in Japan spread rapidly across the North Pacific Ocean and was first observed at the westernmost station on Line P, an oceanographic sampling line extending 1500 km westward of British Columbia (BC), Canada in June 2012. Here, time series measurements of ^{134}Cs and ^{137}Cs in seawater on Line P and on the CLIVAR-P16N 152°W line reveal the recent transport history of the Fukushima radioactivity tracer plume through the northeast Pacific Ocean. During 2013 and 2014 the Fukushima plume spread onto the Canadian continental shelf and by 2015 and early 2016 it reached ^{137}Cs values of 6−8 Bq/m^3 in surface water along Line P. Ocean circulation model simulations that are consistent with the time series measurements of Fukushima ^{137}Cs indicate that the 2015−2016 results represent maximum tracer levels on Line P and that they will begin to decline in 2017−2018. The current elevated Fukushima ^{137}Cs levels in seawater in the eastern North Pacific are equivalent to fallout background levels of ^{137}Cs that prevailed during the 1970s and do not represent a radiological threat to human health or the environment.

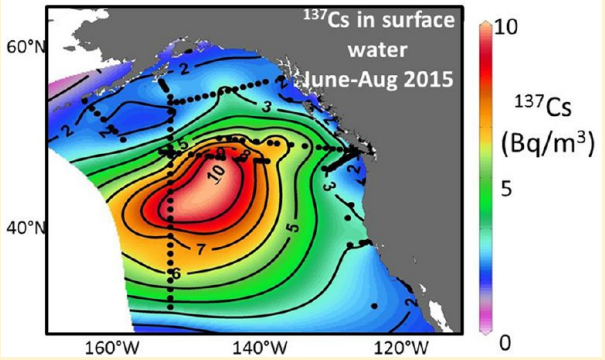

INTRODUCTION

Radioactivity releases from the Fukushima Dai-ichi Nuclear Power Plants (FDNPP; ★, Figure 1) accident represent the largest unplanned discharges of radioactivity that have occurred directly into the ocean.[1−4] The initial discharges occurred from the venting and explosive releases of gases and volatile radionuclides to the atmosphere with greater than 80% being deposited in the ocean.[2] Subsequent, smaller direct discharges to the ocean occurred during emergency cooling efforts as a result of runoff over land,[5] enhanced flow of contaminated groundwater,[6] and the leakage of water from the reactor buildings.[7] Estimates of the total discharges of the most widely studied radionuclide, ^{137}Cs have varied from 3 to 30 PBq, but recent and more precise estimates tend to converge on a range of 15−20 PBq.[2,8,9] The total ^{137}Cs discharges comprise direct oceanic inputs of 3−5 PBq and another 10−15 PBq of ^{137}Cs that were released to the atmosphere and deposited over a broad region of the ocean northeastward of Fukushima (→, Figure 1 inset). These discharges from the FDNPP represent about 25% of the total input of 69 PBq delivered to the North Pacific in the 1950s and 1960s from atmospheric nuclear weapon tests.[9]

The Fukushima radioactivity plume (defined spatially in the ocean by an arbitrary isosurface value) dissipated rapidly in the energetic coastal waters off Japan under the influence of jet-like currents, tidal currents, and mesoscale eddies,[10,11] but a significant remnant was transported eastward by extensions of the Oyashio and Kuroshio systems (Figure 1). The Kuroshio formed a boundary between contaminated surface waters to the north and unaffected waters to the south[12] while the eastward progression of the FDNPP plume was driven by the North Pacific and higher latitude Subarctic Currents. The latter bifurcates as it approaches North America, diverging into the

Received: May 25, 2017
Revised: August 3, 2017
Accepted: August 21, 2017
Published: September 6, 2017

DOI: 10.1021/acs.est.7b02712
Environ. Sci. Technol. 2017, 51, 10494−10502

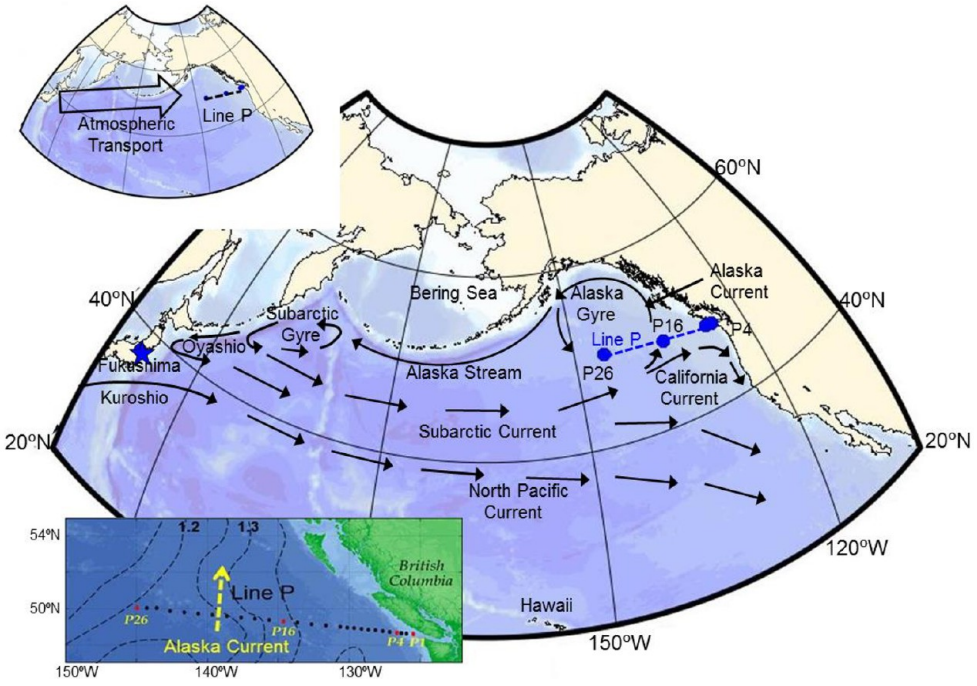

Figure 1. Current systems transported oceanic discharges of radioactivity from Fukushima Daiichi NPP (blue star symbol) eastward across the Pacific and northward across Line P (dashed line) at the eastern edge of the Alaska gyre. Upper inset: Open arrow illustrates general northeastward direction for transport of atmospheric discharges of Fukushima radioactivity. Lower inset: Positions of stations illustrated for Line P. Dashed curves are streamlines whose values (cm) represent the average dynamic height field for 2002−2012 indicating strong northward flow in the Alaska Current (yellow arrow).

northward-flowing Alaska Current and the southward-flowing California Current (Figure 1). The leading edge of the plume advanced at an average speed[8] of 7 km d^{-1} that is consistent with drifter-based estimates of the horizontal spread of the FDNPP plume[13,14] and comparable to zonal geostrophic current velocities in the core of the North Pacific Current.[15]

Ocean circulation models predicted that the major component of the Fukushima radioactivity plume would be almost entirely transported from the western to eastern North Pacific in the five years following the accident and that the highest levels would be first observed off the BC, Canada coast.[16−18] Accordingly, a Canadian monitoring program for the sampling and analysis of seawater for Fukushima radioactivity was initiated shortly after the accident[19] and in the U.S., crowd funding and ships of opportunity were used to monitor the progress and arrival of Fukushima plume along the coast. The results outlined in the present paper are used to delineate water circulation patterns and flow velocity time scales in the eastern North Pacific and to provide insight into the accuracy of global circulation model simulations of Fukushima tracer dispersion.

MATERIALS AND METHODS

The sampling program for the monitoring of the Fukushima radioactivity plume in the eastern North Pacific was anchored by eight missions between June 2011 and Feb. 2016 on the *CCGS John P. Tully* on Line P, two (2014 and 2015) expeditions of the *CCGS S.W. Laurier* in the eastern North Pacific and the 2014 R/V Point Sur and 2015 CLIVAR-P16N cruises. Sample collection in coastal systems was carried out through crowd sourcing programs using citizen scientists in Canada and the U.S. with results posted to the Web sites of InFORM (https://fukushimainform.ca/) and the Woods Hole Oceanographic Institute (WHOI) (http://www.ourradioactiveocean.org/), respectively.

In the Canadian program, large volume (≅60 L) water samples were collected to depths of 1000 m and then passed through potassium cobalt ferrocyanide (KCFC) resin columns to selectively extract Cs isotopes from seawater. Column extraction efficiencies are generally greater than 96% as determined using spiked yield tracers with resin columns arranged in series.[20,21] The isotopes ^{137}Cs and ^{134}Cs were subsequently measured on the oven-dried, KCFC resins in the laboratory using high purity Ge well detectors. All data were decay-corrected to the time, April 6, 2011 of maximum discharges from Fukushima.[1] Detection limits for ^{137}Cs and ^{134}Cs were generally 0.10 Bq/m^3 and 0.13 Bq/m^3, respectively. Detector efficiencies were measured using National Institute of Standards and Technology (NIST) and National Bureau of Sciences (NBS) calibration standards (e.g., NBS 4350B river sediment) and IAEA reference materials. Hydrographic results for the Line P cruises are available at: http://linep.waterproperties.ca. The U.S. open ocean sampling program involved the collection of 20 L seawater samples which were filtered, acidified with nitric acid, and spiked with stable Cs after which radiocesium was extracted using a KNiFC-PAN ion-exchange resin.[22] Resins were dried and gamma counted using methodologies similar to those outlined above. Stable Cs was measured using ICP mass spectrometry to determine and correct for resin extraction efficiencies.

The monitoring of Fukushima radioactivity is simplified by the fact that the initial ^{134}Cs/^{137}Cs activity ratio in Fukushima-derived radioactivity was about 1.[1] Owing to its short half-life ($T_{1/2}$ = 2.1 y), any residual ^{134}Cs in atmospheric fallout from nuclear weapon testing or the Chernobyl accident has decayed in contrast to ^{137}Cs ($T_{1/2}$ = 30 y) for which there is still a

DOI: 10.1021/acs.est.7b02712
Environ. Sci. Technol. 2017, 51, 10494−10502

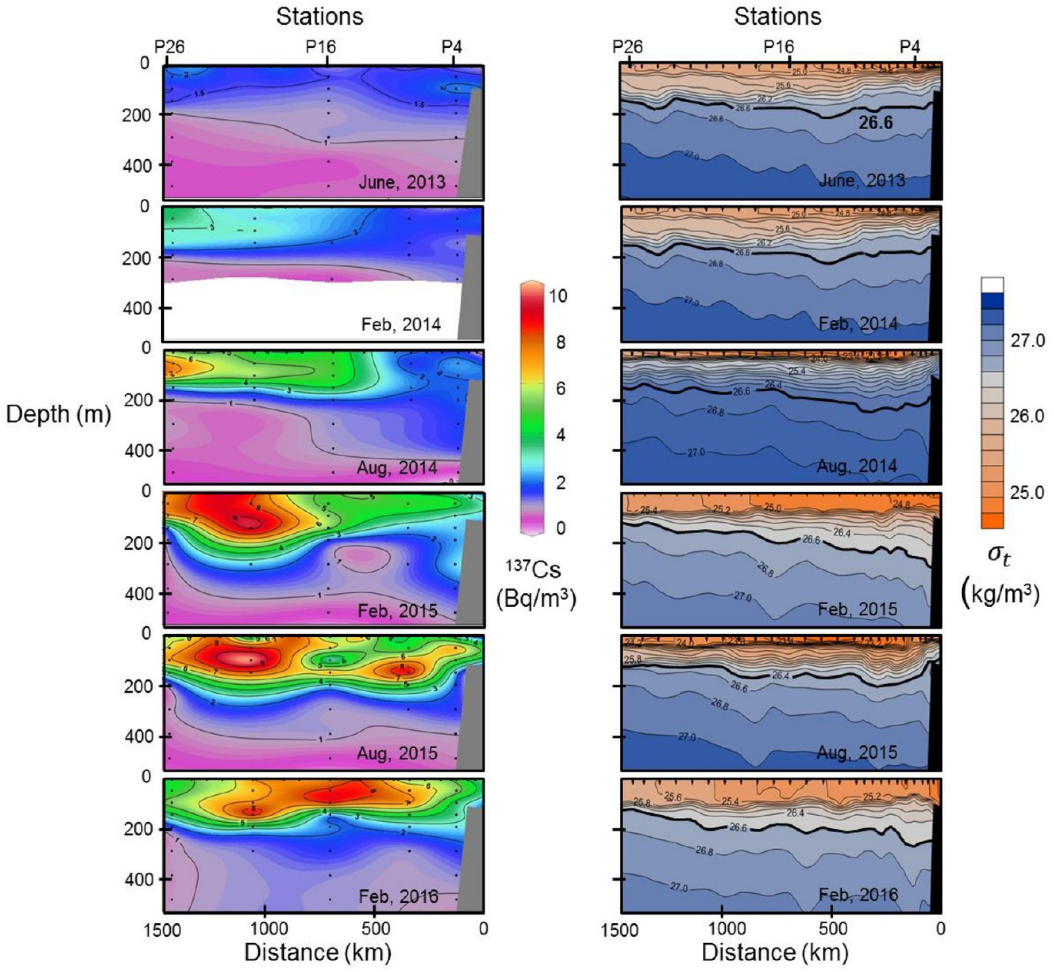

Figure 2. Left panel: Time series of total ^{137}Cs (Fukushima plus fallout) sections show the progressive arrival of the Fukushima signal on Line P between June 2013 and February 2016. Right panel: Time series of density (σ_t) surfaces on Line P with bolded 26.6 isopycnal that outcrops in western North Pacific.

measurable weapon test, fallout background of about 1.2−1.8 Bq/m^3 in surface seawater in the northeastern Pacific. The detection of ^{134}Cs in seawater is therefore an unequivocal "fingerprint" indicator of radiocesium contamination from Fukushima, which is the only large-scale contributor of radioactivity to the Pacific Ocean besides weapon test fallout. The concentration of ^{134}Cs measured in a seawater sample can therefore be decay-corrected to April 6, 2011 to determine the initial ^{134}Cs activity in the sample derived from the Fukushima accident. Since this is also the same as the initial ^{137}Cs activity in the sample derived from Fukushima, this quantity will hereafter be termed the *Fukushima* ^{137}*Cs* activity. It is thereby distinguished from the background, weapon test *fallout* ^{137}*Cs* activity that predates the accident. The *total* ^{137}*Cs* activity is a term used to describe the combined *Fukushima* ^{137}*Cs* plus *fallout* ^{137}*Cs* activities.

RESULTS AND DISCUSSION

Advance of Fukushima Tracer Plume to Line P. Radionuclide measurements on Line P intercept the plume of Fukushima radioactivity advancing along the southern and eastern edges of the Alaska Gyre (Figure 1). Sta. P4 is situated over the continental slope at a water depth of 1300 m while Sta. P26, located at a depth of 4250 m, anchors Line P offshore near the southwestern boundary of the Alaska gyre. Water depth profiles of ^{137}Cs measured at Stas. P4 and P26 at depths up to 1000 m in June 2011, three months after the accident were consistent with weapon test fallout profiles having surface water background levels of 1−2 Bq/m^3 indicating that Fukushima radioactivity transported by ocean currents had not yet arrived in the eastern North Pacific. The first observations of the Fukushima tracer signal were measurements of low levels of ^{134}Cs in the upper 100 m at Sta. P26 in June 2012.[19] By June 2013, ^{134}Cs from Fukushima was detectable in surface water at most stations sampled on Line P at levels of about 1−2 Bq/m^3 (decay-corrected to time of Fukushima accident), thereby providing the first evidence for the arrival of the Fukushima radioactivity plume in western North American continental waters. In 2013, ^{134}Cs was detectable to a depth of 100 m of the water column, matching the maximum depth of the winter mixed layer in the eastern North Pacific at Sta. P26.[23]

The June 2013, Line P section for total ^{137}Cs (Fukushima plus fallout ^{137}Cs) is illustrated in Figure 2 (upper left panel). Through February and August, 2014 total ^{137}Cs concentrations in surface water at the western end of Line P (Stas. P16−P26) increased steadily to levels >5 Bq/m^3, while much smaller ^{137}Cs increases were observed at the eastern end of Line P proximal to the continental shelf (Figure 2). During 2014, ^{137}Cs levels began to increase at water depths of 150−200 m that extend well below the surface mixed layer, particularly on the western

DOI: 10.1021/acs.est.7b02712
Environ. Sci. Technol. 2017, 51, 10494−10502

end of Line P. These observations indicate that Fukushima ^{137}Cs had been injected into the pycnocline upstream of Line P in the western North Pacific where winter mixed layer depths are deeper than in the more surface stratified regime of the Northeast Pacific. Between August 2014 and February 2015 the ^{137}Cs plume began to advance shoreward and to descend to depths below 200 m. By August 2015 the total ^{137}Cs plume had progressed to the eastern side of Line P and by February 2016 had increased in concentration to values in excess of 8 Bq/m^3 at central locations (Figure 2).

Line P density sections illustrated in Figure 2 (right-hand panel) exhibit several features that reflect processes governing ^{137}Cs transport. The eastward deepening of the ^{137}Cs signal on Line P over time reflects tracer spreading with minimal diapycnal mixing in a shoreward direction owing to ^{137}Cs concentration gradients on the large-scale, downward tilting isopycnal surfaces. The σ_t = 26.6 kg/m^3 isopycnal (bolded in Figure 2) corresponds to North Pacific Intermediate Water (NPIW) that outcrops in regions northeast of Japan that also received significant atmospheric inputs of Fukushima fallout.[24] NPIW is formed on time scales of 1−2 years[25] by winter mixing in the subarctic gyre of the western North Pacific (Figure 1) and takes 5−7 years to flow along the 26.5−26.8 isopycnals (at water depths of 100−200 m) to Sta. P26 on Line P.[26] These values are similar to transit time inferences[27] for NPIW flow based on minimum AOU (Apparent Oxygen Utilization) measurements at Sta. P26. The eastward spreading of Fukushima ^{137}Cs in NPIW from the subarctic gyre to Line P could explain the arrival of Fukushima ^{137}Cs at depths of 100−200 m at Sta. P26 by 2014 if these spreading rates were slightly faster than those[25,26] cited above.

Subsurface transport of the Fukushima signal has been extensively documented in the western Pacific. In 2013, Yoshida et al.[28] measured Fukushima ^{137}Cs at 600 m near the 26.5 isopycnal surface on a 30°N longitudinal transect near 180° which they hypothesized may be the result of Fukushima isotopes being directly discharged into the ocean near the NPIW formation region and transported to the mid depth subtropical gyre following NPIW pathways. Fukushima ^{137}Cs has also been observed[8,28,29] in several mode waters including Central Mode Water (CMW) and Subtropical Mode Water (STMW) formed in subduction areas north and south, respectively of the Kuroshio.[30] The southernmost (25−30°N) region of subduction, where STMW forms ($\sigma_t \cong$ 25 kg/m^3) likely entrained only the fallout portion of Fukushima ^{137}Cs, since the direct release occurred farther north. However, subduction zones for lighter CMW (LCMW, $\sigma_t \cong$ 26 kg/m^3 formed within 30−37.5°N) and denser CMW (DCMW, $\sigma_t \cong$ 27 kg/m^3 formed within 37.5−45°N) are sufficiently far north that ^{137}Cs can be entrained into the interior ocean from both direct releases and atmospheric deposition.[8] In fact, a strong (~10 Bq/m^3), subsurface (50−300 m) Fukushima ^{137}Cs signal was observed southwest (152°W, 43°N) of Line P during the 2015 CLIVAR-P16N cruise that is predominately carried by DCMW (A. Macdonald, Pers. comm.) suggesting that tracer transport associated with DCMW contributes to Fukushima ^{137}Cs inventories below 100 m on Line P.

At smaller, continental shelf scales an additional factor that influences ^{137}Cs distributions on Line P is upwelling over the BC continental slope and outer shelf caused by the prevailing, along shore, southward winds during summer months. This process is reflected in density sections in Figure 2 by upward tilting isopycnals adjacent to the shelf break that were observed on August cruises. Upwelling is accompanied by a weak seaward flow in the surface Ekman layer and by a strong surface-intensified southeastward flow associated with the wind-induced shelf-break current centered near the 200 m depth contour. Eddies and lateral turbulent mixing associated with these currents transport fresher, subsurface coastal water over the shelf which tends to have lower ^{137}Cs concentrations derived mainly from weapon test fallout and thereby prevents the surface Fukushima radionuclide plume from reaching nearshore regions. In addition, the mixing of recently upwelled waters (having low ^{137}Cs levels from weapon test fallout) with the offshore plume (higher ^{137}Cs levels from Fukushima), followed by subduction and subsequent recirculation into the coastal upwelling can produce subsurface tracer maxima close to the shelf as observed in ^{137}Cs panels (Figure 2) for August 2014 and 2015. The deeper ^{137}Cs signal below depths of 300 m in each panel represents a residual weapon test fallout signal that has accumulated over previous years by ocean interior transport on isopycnal surfaces.

The eastward advance of the Fukushima ^{137}Cs signal in surface water along Line P is illustrated in Figure 3 by an

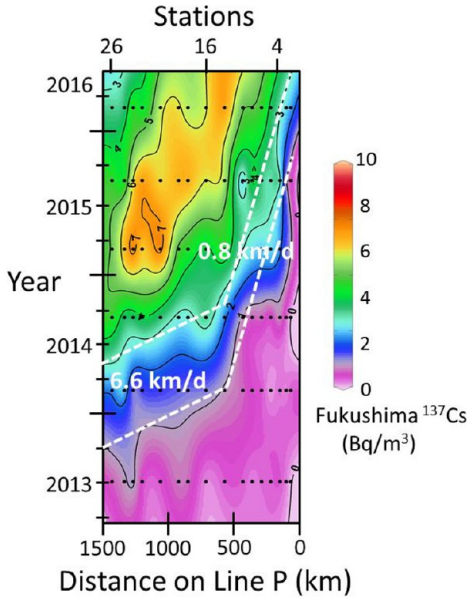

Figure 3. Landward transport of the Fukushima tracer signal is illustrated by a Hovmöller diagram (time versus distance) of mean Fukushima ^{137}Cs concentrations (Bq/m^3) in the upper 150 m along Line P. The value of the slope of a given iso-concentration boundary (white dashed lines) gives the reciprocal of the inshore spreading velocity of the Fukushima signal along Line P.

Hovmöller diagram (time versus distance from the coast) for mean Fukushima ^{137}Cs (Bq/m^3) in the upper 150 m. The slope of a given iso-concentration boundary (white dashed lines) represents the inverse of the inshore flow velocity of the Fukushima signal. During 2013−2014, the Fukushima signal advanced eastward at a speed of 6.6 km/d between stations 26 and 15, based on the 1−3 Bq/m^3 iso-concentration curves (Figure 3). However, further eastward advance from Sta. 15 to Sta. 4 occurred at a much slower rate of 0.8 km/d (Figure 3). The principal component of the Fukushima plume arrived at Line P in 2014−2015 during which the eastward transport rate of the Fukushima signal on the western end of Line P decreased

DOI: 10.1021/acs.est.7b02712
Environ. Sci. Technol. 2017, 51, 10494−10502

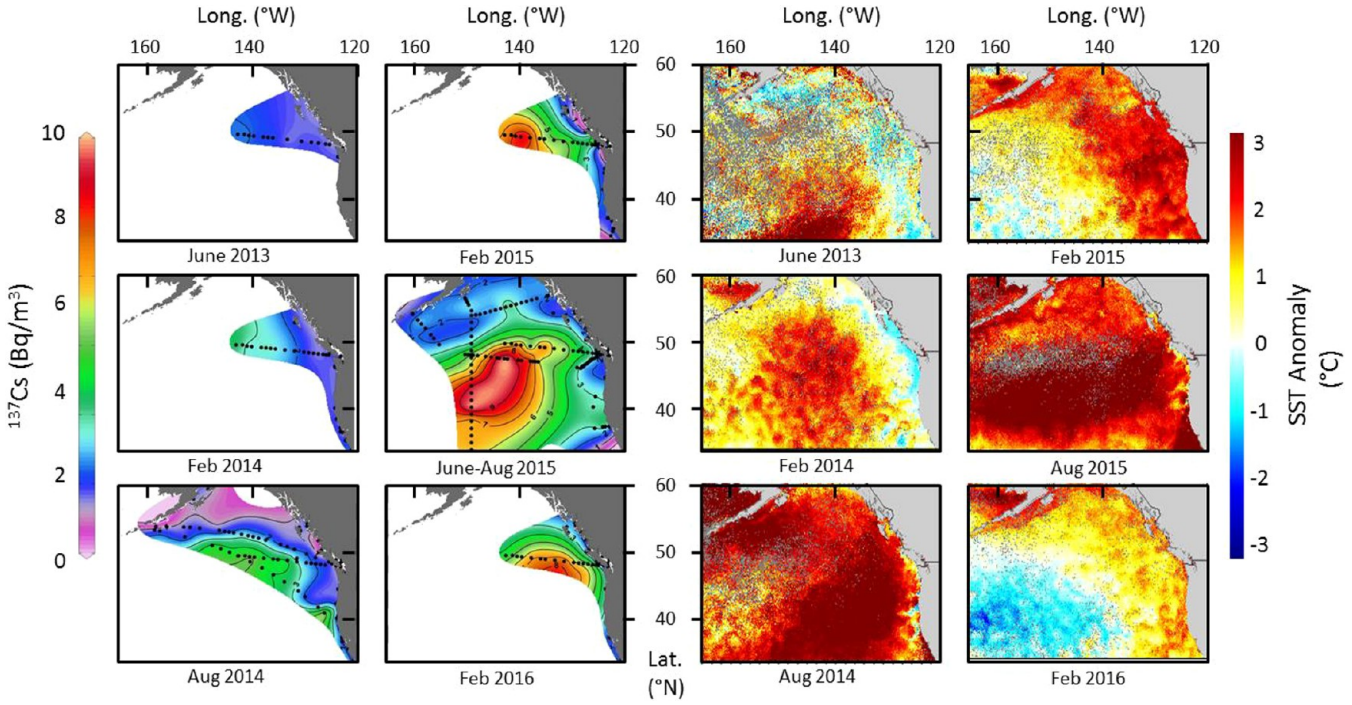

Figure 4. Left two columns: total ^{137}Cs surface water distributions for June 2013 to Feb 2016 show spatial evolution of the Fukushima plume as it nears the coastline. Right two columns: SST anomaly distributions (http://coastwatch.pfel.noaa.gov/data.html) for same time period outline the development of the warm "blob" which occupies the same water masses as Fukushima tracer patch.

slightly, but the same slow flow rate of 0.8 km/d was observed eastward from Sta. 15.

The Fukushima ^{137}Cs plume took about two years to be transported 6000 km across the Pacific Ocean in the North Pacific Current to Sta. 26 at a speed of 7 km/d[8] and then advanced eastward across the Alaska Current from Sta. P26 to Sta. P15 at 5−7 km/d. However, the continued progression of the signal eastward from Sta. P15 to the continental shelf occurred at the sharply reduced rate of 0.8 km/d. There are several factors contributing to this reduced flow rate in the onshore transport of the tracer signal. Line P is situated in the vicinity of the bifurcation of the North Pacific Current, where the large-scale circulation diverges into the northward flowing Alaska Current and the southward flowing California Current (Figure 1). These flows are subject to pronounced variability on interannual to decadal time scales. Time-averaged streamlines representing the mean dynamic height field for 2002−2012 calculated from ARGO float data (http://www.meds-sdmm.dfo-mpo.gc.ca/isdm-gdsi/argo/canadian-products/index-eng.html) are illustrated in Figure 1 (inset). The mean streamlines are concentrated on the western end of Line P (seaward of Sta. P15), which on average intercepts the northward geostrophic transport of the Alaska Current with flow speeds of 5−10 km/d. The streamlines diverge markedly on the eastern end of Line P, which lies generally within the bifurcation zone. The flow in this region is highly variable, and mean currents are weak and difficult to define.[15] Indeed, this region with strong seasonal variability constitutes the transition zone between the quasi-permanent coastal upwelling to the south (California coast) and the dominant downwelling to the north. The decreasing ^{137}Cs tracer levels in the surface mixed layer eastward along Line P (Figure 2) therefore represent a transition from higher levels in the northward flowing core of the Fukushima tracer plume to lower levels in the weaker, transitional flow field of the bifurcation zone. This slower eastward flow of the Fukushima signal onto the shelf is illustrated by the reduced spreading velocity between Sta. 15 and Sta. 4 inferred from the ^{137}Cs iso-concentration curves in Figure 3.

A second factor in the onshore flow of the Fukushima signal is related to the large scale atmospheric circulation in 2013−2015. This factor is addressed in Figure 4, where the left-hand time series panels show areal time series distributions for total ^{137}Cs (Fukushima plus weapon test fallout ^{137}Cs) in surface water between 2013 and 2016 for samples collected in the offshore and coastal monitoring programs (InFORM and WHOI) noted in the Materials and Methods. The right-hand panels (Figure 4) show sea surface temperature (SST) anomalies for the same geographical regions and sampling time frames.

During the winter of 2013−2014 a large pool of unusually warm water was observed in the south central Gulf of Alaska.[31] Within the upper ∼100 m of the ocean, temperatures were as much as 2.5 °C (4.0 °F) above average in February 2014 creating a warm, sea surface temperature (SST) anomaly that became popularly known as the warm "blob".[31] The SST anomaly had its origins in the preceding winter of 2012−2013, but its signature became considerably stronger in 2013−2014 as illustrated by the area of the high sea surface temperature (SST) anomalies (departures from the 1981−2010 mean) which in February 2014 intersected the western end of Line P and extended southward to 35 N° (Figure 4; right-hand panels). The formation of the SST anomaly was related to an overlying region of unusually persistent and record-high atmospheric pressure that for the winter of 2013−2014 hovered over the eastern North Pacific, deflecting the storm track northward away from the West Coast.[32] With the ridge in place the West Coast's typical northwest winds which produce mechanical mixing and upwelling, slackened, thereby allowing

DOI: 10.1021/acs.est.7b02712
Environ. Sci. Technol. 2017, 51, 10494−10502

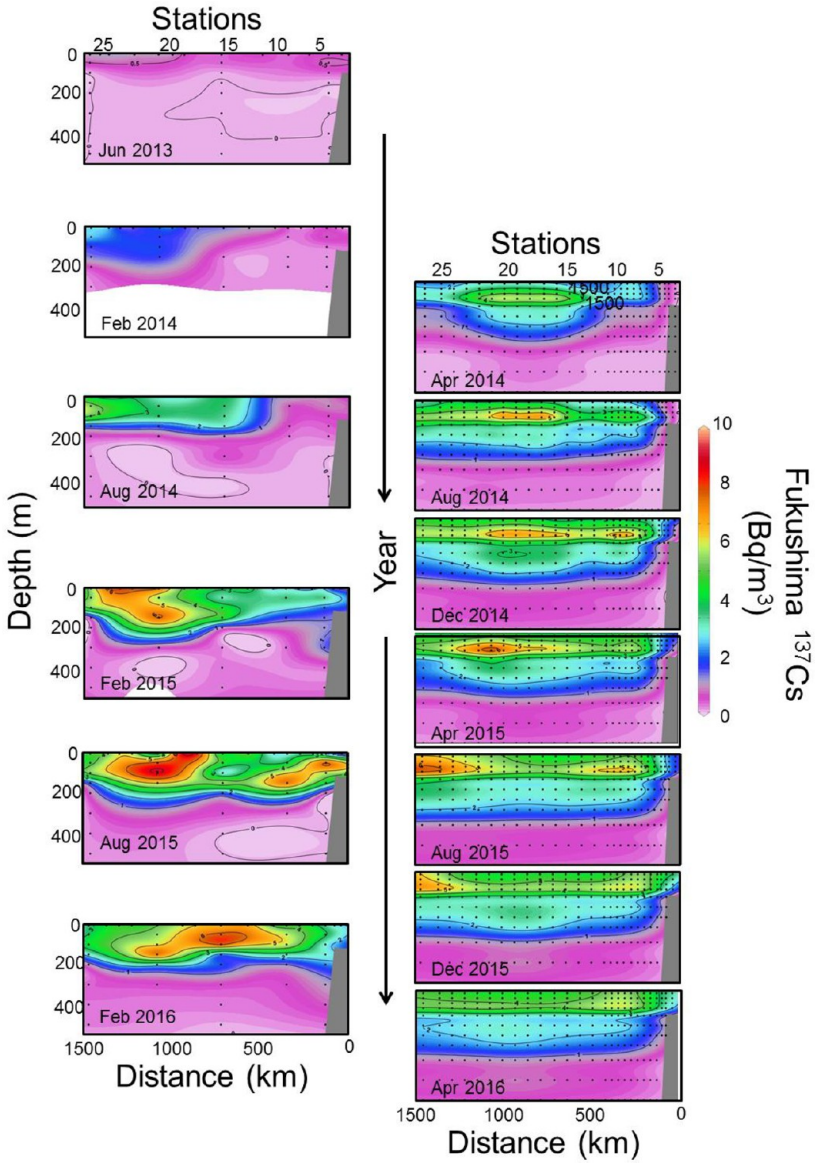

Figure 5. Left Panel: Measured Line P time series sections for Fukushima ^{137}Cs. Right Panel: Line P ^{137}Cs time series simulations[16,17] are generally consistent with main features of the measured results.

the surface layer water to retain large quantities of heat (Figure 4, February and August 2014 SST panels). During the winter of 2014−2015 the high atmospheric pressure system weakened, and the SST anomaly shifted southward and evolved into a configuration known as the Arc Pattern.[33] The high atmospheric pressure ridge had completely dissipated by the winter of 2015−2016 resulting in a return of the normal storm track and the usual pattern of surface layer mixing giving the relatively even areal SST distribution evident in the February 2016 panel of Figure 4.

The ^{137}Cs signal became an incidental proxy radiochemical tracer for the warm SST anomaly or "blob". The areal distribution of total ^{137}Cs derived from surface water measurements for August 2014 outlines (Figure 4) the northern component of a large pool of water labeled by ^{137}Cs levels in excess of 5 Bq/m^3 that is nearly spatially congruent with the spatial configuration of the SST anomaly. Despite this large offshore signal, Fukushima ^{137}Cs was not observed in August 2014 in seawater collected at the coastal stations operated by the InFORM and WHOI monitoring programs. However, as the ridge of anomalously high atmospheric pressure over the NE Pacific began to dissipate during the winter of 2014−2015, partly in response to weak El Niño-like warming along the equator,[33] both warm SST anomaly water and Fukushima ^{137}Cs sporadically and concurrently reached the Canadian coastline (February 2015 SST panel, Figure 4) as first observed at Ucluelet, BC in February, 2015 (https://fukushimainform.ca/about/informal-e-news-archives/). By August 2015 Fukushima ^{137}Cs had been detected at multiple locations along the Canadian and U.S. coastlines as the SST anomaly pattern broadened and shifted southeastward. By February 2016, the high atmospheric pressure ridge had dissipated and both the anomalously warm water and the Fukushima ^{137}Cs signal had spread southward along the U.S. coastline to California (http://www.ourradioactiveocean.org/).

Comparison of Measured Fukushima ^{137}Cs Distributions to Model Simulation. Various global ocean circulation models[8,16−18] have been used to simulate the long-term

DOI: 10.1021/acs.est.7b02712
Environ. Sci. Technol. 2017, 51, 10494−10502

spreading of the Fukushima signal across the North Pacific Ocean. The Rossi et al.[16,17] model used Lagrangian particles within the regional eddy-resolving, Ocean General Circulation Model for the Earth Simulator (OFES) to evaluate multi-decadal transport of the Fukushima plume along surface and subsurface pathways. They projected the arrival of the Fukushima plume at Sta. P26 on Line P to occur in early 2014, in general agreement with the present observations (Figure 2). In addition, their simulated ^{137}Cs concentrations after correction[17] exhibited a good fit with data measured along the International Date Line (180°) in 2012.[8]

The Rossi et al.[17] simulations of the Fukushima ^{137}Cs time series sections on Line P are compared to the experimental results in Figure 5. The model simulations are in agreement with experimental observations with two key exceptions. First, the model predicts that the leading edge of the Fukushima signal would be initially observed centrally on Line P near Sta. P16 (Figures 5 and 6). The experimental results (Figures 4–6)

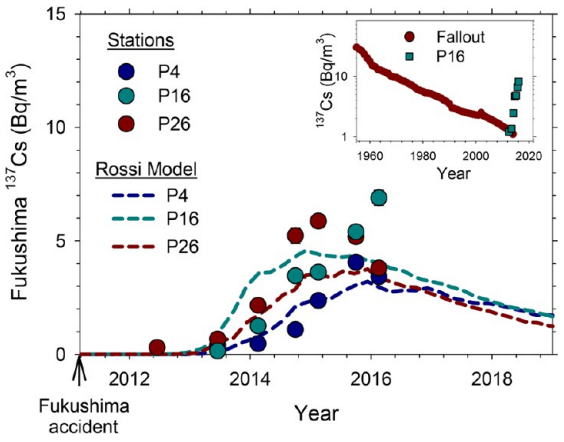

Figure 6. Time series for mean measured Fukushima ^{137}Cs concentrations in upper 150 m at Stas. P4, P16, and P26 on Line P are compared to model simulations.[16,17] Inset: ^{137}Cs time series for fallout in N. Pacific[37,38] and total ^{137}Cs (fallout plus Fukushima) in upper 150 m at Sta. 16.

reveal that the eastward spreading signal actually first encountered Line P at the westernmost station, Sta. P26. The likely explanation for this data-model inconsistency stems from the model[16,17] assumption that radioactivity releases occurred solely by direct discharges from the Fukushima plant into the ocean. This assumption is challenged by measurements of ^{137}Cs levels >10 Bq/m^3 in April–June 2011 at locations between 40°N and 50°N in the North Pacific.[24] These observations were both too distant from Fukushima and made too soon after the accident to be explained by surface current transport from Fukushima, thereby indicating the presence of an additional, more northerly, atmospheric transport pathway for Fukushima fallout. Furthermore, model simulations[34] with input functions combining direct discharges and atmospheric deposition have successively reproduced observed Fukushima ^{134}Cs ocean distributions during 2011–2014. It follows that the initial rapid advance of a component of the Fukushima signal through the atmosphere (as illustrated approximately in Figure 1) and its concurrent deposition in the surface ocean is responsible for its arrival at Sta. P26 earlier than predicted by the Rossi et al.[16,17] model simulations.

The second model-data discrepancy is associated with model simulations showing the descent of the Fukushima signal to 300 m by the time it arrives on Line P (Figure 5), in contrast to the experimental results indicating negligible transport of Fukushima ^{137}Cs had occurred below 250 m by 2016. This inconsistency derives from model predictions of more rapid vertical subduction and eastward spreading of Fukushima ^{137}Cs along the deeper isopycnal surfaces at 300 m ($\sigma_t \cong 26.8–26.9$ kg/m^3) than that actually observed. This result is associated with the extension of the surface plume, its concentration, and the duration of its transit through the deep convection zones as it is directly linked to the model adoption of a source function neglecting atmospheric discharges. Most of the actual ^{137}Cs deposition occurred during the first 2 months after the accident and over a large portion of the Northwestern Pacific (~30–45°N, east to 180°) congruent with formation regions for DCMW and LCMW.[35] The Rossi et al. model may have underestimated the subduction rate of ^{137}Cs into DCMW and LCMW during the first subduction event (during winter-spring 2011), but then overestimated it in subsequent years (2012–2015). The positive bias of the model at depths spanning 200–400 m along line P seems to support the hypothesized overestimated ^{137}Cs subduction in mode waters when neglecting atmospheric deposition. However, the capability of the model to reproduce realistic trajectories and timing of mode-water flow on deep pathways could also play a key role in this regional mismatch, especially as ventilation rates of intermediate and deep waters are known to have substantial biases in large-scale ocean models.[36]

Line P time series for mean, surface mixed layer (0–150 m) Fukushima ^{137}Cs concentrations at Stas. P4, P16, and P26 are compared with the results of the model simulation[16,17] in Figure 6. As noted above, the model time series for Fukushima ^{137}Cs slightly lags the measured values at the westernmost location, Sta. P26. Measured values of Fukushima ^{137}Cs at Sta. P16 during Aug 2015–Feb 2016 are higher than the model values, but more recent measurements (J. Smith, Pers. comm.) at Sta. 16 in 2016–2017 support model predictions of a post-2015 decreasing trend in the Fukushima ^{137}Cs concentration. The model is in good agreement with the measured Fukushima ^{137}Cs time series at the shelf edge location, Sta. P4 where confounding factors such as the early atmospheric delivery of Fukushima ^{137}Cs and enhanced stratification associated with warm SST anomalies may have had minimal impact. Generally, the model-data comparison indicates that Line P surface mixed layer Fukushima ^{137}Cs concentrations were at their maxima in 2015–2016 and are predicted to decline during 2017–2018.

Given that the ^{137}Cs weapon test fallout background averaged 1.5 Bq/m^3 in surface water on Line P, levels of Fukushima ^{137}Cs of about 7 Bq/m^3 measured on Line P in 2016 can be viewed as increasing the weapon test fallout background by a factor of about 5. Comparison with the history of atmospheric fallout in surface water[37,38] in the North Pacific (inset, Figure 6) indicates that total ^{137}Cs values (Fukushima plus weapon test fallout ^{137}Cs) of 8.5 Bq/m^3 measured at Sta. 16 have returned ^{137}Cs levels in specific water masses such as the Alaska Current to those fallout levels that prevailed during the early 1970s. However, these concentrations of ^{137}Cs in the Northeast Pacific Ocean are well below Canadian guidelines for drinking water quality for which the maximum acceptable concentration (MAC) of ^{137}Cs in drinking water is 10 000 Bq/m^3 and do not represent a radiological threat to human health or the environment.[39]

DOI: 10.1021/acs.est.7b02712
Environ. Sci. Technol. 2017, 51, 10494–10502

AUTHOR INFORMATION

Corresponding Author

*E-mail: john.smith@dfo-mpo.gc.ca (J.N.S.).

ORCID

John N. Smith: 0000-0003-3628-444X

Vincent Rossi: 0000-0001-7291-0415

Notes

The authors declare no competing financial interest.

ACKNOWLEDGMENTS

The authors wish to thank the officers and crews of the *CCGS John P. Tully*, *CCGS Laurier* (CLIVAR), K. Purdon, L. McKay, and S. Kowallik for their assistance in sample collection and G. Folwarczna (DFO) for her laboratory assistance. J.S., J.T.C., J.C., and J.K. acknowledge funding support from MEOPAR for the InFORM network. K.B. and A.M. acknowledge funding support from the National Science Foundation (grant #OCE-1356630 and #OCE-1437015) for the GO-SHIP/CLIVAR P16N cruise in 2015, the Deerbrook Charitable Trust for support of KBs salary, and more than 350 individuals and groups who contributed to the Our Radioactive Ocean crowd funding campaign. We also wish to thank R. Brown and R. Thomson for their insights and helpful comments. This research includes computations using the Linux computational cluster Katana supported by Faculty of Science, UNSW Australia.

REFERENCES

(1) Buesseler, K.; Aoyama, M.; Fukasawa, M. Impacts of the Fukushima nuclear power plants on marine radioactivity. *Environ. Sci. Technol.* **2011**, *45*, 9931−9935.

(2) Buesseler, K.; Dai, M.; Aoyama, M.; Benitez-Nelson, C.; Charmasson, S.; Higley, K.; Maderich, V.; Masque, P.; Oughton, D.; Smith, J. N.; Morris, P. J. Fukushima Daiichi−derived radionuclides in the ocean: Transport, fate, and impacts. *Annu. Rev. Mar. Sci.* **2017**, *9*, 173−203.

(3) Charette, M. A.; Breier, C. F.; Henderson; Pike, S. M.; Rypina, I. I.; Jayne, S. R.; Buesseler, K. Radium-based estimates of cesium isotope transport and total direct ocean discharges from the Fukushima Nuclear Power Plant accident. *Biogeosciences* **2013**, *10*, 2159−2167.

(4) Inomata, Y.; Aoyama, M.; Tsubono, T.; Tsumune, D.; Hirose, K. Spatial and temporal distributions of ^{134}Cs and ^{137}Cs derived from the TEPCO Fukushima Daiichi Nuclear Power Plant accident in the North Pacific Ocean by using optimal interpolation analysis. *Environ. Sci.: Processes Impacts* **2016**, *18* (1), 126−136.

(5) Evrard, O.; Laceby, J. P.; Lepage, H.; Onda, Y.; Cerdan, O.; Ayrault, S. Radiocesium transfer from hillslopes to the Pacific Ocean after the Fukushima nuclear power plant accident: a review. *J. Environ. Radioact.* **2015**, *148*, 92−110.

(6) Marui, A.; Gallardo, A. H. Managing groundwater radioactive contamination at the Daiichi Nuclear Plant. *Int. J. Environ. Res. Public Health* **2015**, *12* (7), 8498−8503.

(7) Castrillejo, M.; Casacuberta, N.; Breier, C. F.; Pike, S. M.; Masque, P.; Buesseler, K. O. Reassessment of ^{90}Sr, ^{137}Cs, and ^{134}Cs in the coast off Japan derived from the Fukushima Dai-Ichi nuclear accident. *Environ. Sci. Technol.* **2016**, *50*, 173−180.

(8) Aoyama, M.; Hamajima, Y.; Hult, M.; Uematsu, M.; Oka, E.; Tsumune, D.; Kumamoto, Y. ^{134}Cs and ^{137}Cs in the North Pacific Ocean derived from the March 2011 TEPCO Fukushima Dai-ichi Nuclear Power Plant accident, Japan. Part one: surface pathway and vertical distributions. *J. Oceanogr.* **2016**, *72*, 53.

(9) Aoyama, M.; Kajino, M.; Tanaka, T. Y.; Sekiyama, T. T.; Tsumune, D.; Tsubono, T.; Hamajima, Y.; Inomata, Y.; Gamo, T. ^{134}Cs and ^{137}Cs in the North Pacific Ocean derived from the March 2011 TEPCO Fukushima Dai-ichi Nuclear Power Plant accident, Japan. Part two: estimation of ^{134}Cs and ^{137}Cs inventories in the North Pacific Ocean. *J. Oceanogr.* **2016**, *72*, 67.

(10) Masumoto, Y.; Miyazawa, Y.; Tsumune, D.; Tsubono, T.; Kobayashi, T.; Kawamura, H.; Estournel, C.; Marsaleix, P.; Lanerolle, L.; Mehra, A.; Garraffo, Z. D. Oceanic dispersion simulations of ^{137}Cs released from the Fukushima Daiichi nuclear power plant. *Elements* **2012**, *8*, 207−212.

(11) Tsumune, D.; Tsubono, T.; Aoyama, M.; Uematsu, M.; Misumi, K.; Maeda, Y.; Yoshida, Y.; Hayami, H. One-year, regional-scale simulation of ^{137}Cs radioactivity in the ocean following the Fukushima Dai-ichi Nuclear Power Plant accident. *Biogeosciences* **2013**, *10*, 5601−5617.

(12) Buesseler, K.; Jayne, S. R.; Fisher, N. S.; Rypina, I. I.; Baumann, H.; Baumann, Z.; Breier, C. F.; Douglass, E. M.; George, J.; Macdonald, A. M.; Miyamoto, H.; Nishikawa, J.; Pike, S. E.; Yoshida, S. Fukushima-derived radionuclides in the ocean and biota off Japan. *Proc. Natl. Acad. Sci. U. S. A.* **2012**, *109* (16), 5984−5988.

(13) Rypina, I. I.; Jayne, S. R.; Yoshida, S.; Macdonald, A. M.; Douglass, E.; Buesseler, K. Short-term dispersal of Fukushima-derived radionuclides off Japan: modeling efforts and model-data intercomparison. *Biogeosciences* **2013**, *10*, 4973−90.

(14) Rypina, I. I.; Jayne, S. R.; Yoshida, S.; Macdonald, A. M.; Buesseler, K. Drifter-based estimate of the 5 year dispersal of Fukushima-derived radionuclides. *J. Geophys. Res.* **2014**, *119*, 8177−93.

(15) Cummins, P. F.; Freeland, H. J. Variability of the North Pacific Current and its bifurcation. *Prog. Oceanogr.* **2007**, *75*, 253−265.

(16) Behrens, E.; Schwarzkopf, F. U.; Lubbecke, J. F.; Boning, C. W. Model simulations on the long-term dispersal of ^{137}Cs released into the Pacific Ocean off Fukushima. *Environ. Res. Lett.* **2012**, *7*, 034004.

(17) Rossi, V.; Van Sebille, E.; Sen Gupta, A.; Garçon, V.; England, M. H. Multi-decadal projections of surface and interior pathways of the Fukushima Cesium-137 radioactive plume. *Deep Sea Res., Part I* **2013**, *80*, 37−46.

(18) Rossi, V.; Sebille, E. V.; Gupta, A. S.; Garçon, V.; England, M. H. Corrigendum to "Multi-decadal projections of surface and interior pathways of the Fukushima Cesium-137 radioactive plume" [*Deep-Sea Res. I* 80 (2013) 37−46]. *Deep Sea Res., Part I* **2014**, *93*, 162−164.

(19) Smith, J. N.; Brown, R. M.; Williams, W. J.; Robert, M.; Nelson, R. N.; Moran, S. B. Arrival of the Fukushima radioactivity plume in North American continental waters. *Proc. Natl. Acad. Sci. U. S. A.* **2015**, *112* (5), 1310−1315.

(20) Smith, J. N.; Ellis, K. M.; Jones, E. P. Cesium-137 transport into the Arctic Ocean through Fram Strait. *J. Geophys. Res.* **1990**, *95* (C2), 1693−1701.

(21) Smith, J. N.; McLaughlin, F. A.; Smethie, W. M., Jr.; Moran, S. B.; Lepore, K. Iodine-129, ^{137}Cs, and CFC-11 tracer transit time distributions in the Arctic Ocean. *J. Geophys. Res.* **2011**, *116*, 116.

(22) Breier, C. A. F.; Pike, S. M.; Sebesta, F.; Tradd, K.; Breier, J. A.; Buesseler, K. O. New applications of KNiFC-PAN resin for broad scale monitoring of radiocesium following the Fukushima Dai-ichi nuclear disaster. *J. Radioanal. Nucl. Chem.* **2016**, *307*, 2193.

(23) Thomson, R. E.; Fine, I. A diagnostic model for mixed layer depth estimation with application to Ocean Station P in the Northeast Pacific. *J. Phys. Ocean.* **2009**, *39*, 1399−1415.

(24) Aoyama, M.; Uematsu, M.; Tsumune, D.; Hamajima, Y. Surface pathway of radioactive plume of TEPCO Fukushima NPP1 released ^{134}Cs and ^{137}Cs. *Biogeosciences* **2013**, *10*, 3067−3078.

(25) Shimizu, Y.; Iwao, T.; Yasuda, I.; Ito, S.; Watanabe, T.; Uehara, K.; Shikama, N.; Nakano, T. Formation process of North Pacific Intermediate Water revealed by profiling floats set to drift on 26.7σ_θ isopycnal surface. *J. Oceanogr.* **2004**, *60*, 453−462.

(26) Ueno, H.; Yasuda, I. Intermediate water circulation in the North Pacific subarctic and northern subtropical regions. *J. Geophys. Res.* **2003**, *108* (C11), 3348.

(27) Whitney, F. A.; Freeland, H. J.; Robert, M. Persistently declining oxygen levels in the interior waters of the eastern subarctic Pacific. *Prog. Oceanogr.* **2007**, *75*, 179−199.

(28) Yoshida, S.; Macdonald, A. M.; Jayne, S. R.; Rypina, I. I.; Buesseler, K. O. Observed eastward progression of the Fukushima

DOI: 10.1021/acs.est.7b02712
Environ. Sci. Technol. 2017, 51, 10494−10502

^{134}Cs signal across the North Pacific. *Geophys. Res. Lett.* **2015**, *42*, 7139−7147.
(29) Kaeriyama, H.; Shimizu, Y.; Setou, T.; Kumamoto, Y.; Okazaki, M.; Ambe, D.; Ono, T. Intrusion of Fukushima-derived radiocaesium into subsurface water due to formation of mode waters in the North Pacific. *Sci. Rep.* **2016**, *6*, 22010.
(30) Oka, E.; Qiu, B. Progress of North Pacific mode water research in the past decade. *J. Oceanogr.* **2012**, *68*, 5−20.
(31) Bond, N. A.; Cronin, M. F.; Freeland, H.; Mantua, N. Causes and impacts of the 2014 warm anomaly in the NE Pacific. *Geophys. Res. Lett.* **2015**, *42* (9), 3414−3420.
(32) Hartmann, D. L. Pacific sea surface temperature and the winter of 2014. *Geophys. Res. Lett.* **2015**, *42*, 189410.1002/2015GL063083.
(33) Di Lorenzo, E.; Mantua, N. Multi-year persistence of the 2014/15 North Pacific marine heatwave. *Nat. Clim. Change* **2016**, *6* (11), 1042.
(34) Tsubono, T.; Misumi, K.; Tsumune, D.; Bryan, F. O.; Hirose, K.; Aoyama, M. Evaluation of radioactive cesium impact from atmospheric deposition and direct release fluxes into the North Pacific from the Fukushima Daiichi nuclear power plant. *Deep Sea Res., Part I* **2016**, *115*, 10−21.
(35) Oka, E.; Qiu, B.; Kouketsu, S.; Uehara, K.; Suga, T. Decadal seesaw of the Central and Subtropical Mode Water formation associated with the Kuroshio Extension variability. *J. Oceanogr.* **2012**, *68*, 355−360.
(36) Dutay.; et al. Evaluation of ocean model ventilation with CFC-11: comparison of 13 global ocean models. *Ocean Model.* **2002**, *4* (2), 89−120.
(37) Aoyama, M.; Hirose, K. Artificial radionuclides database in the Pacific Ocean: HAM database. *Sci. World J.* **2004**, *4*, 200−215.
(38) Kaeriyama, H. Oceanic dispersion of Fukushima-derived radioactive cesium: a review. *Fish. Oceanogr.* **2017**, *26* (2), 99−113.
(39) Fisher, N. S.; Beaugelin-Seiller, K.; Hinton, T. G.; Baumann, Z.; Madigan, D. J.; Garnier-LaPlace, J. An evaluation of radiation doses and associated risk from the Fukushima nuclear accident to marine biota and human consumers of seafood. *Proc. Natl. Acad. Sci. U. S. A.* **2013**, *110*, 10670−10675.

DOI: 10.1021/acs.est.7b02712
Environ. Sci. Technol. 2017, 51, 10494−10502